# Simulation of joint position response of 60 kg payload 4-Axes SCARA configuration manipulator taking dynamical effects into consideration

G. Purkayastha, S. Datta, S. Nandy, S.N. Shome
Robotics & Automation Group,
Central Mechanical Engineering Research Institute,
M.G. Avenue, Durgapur, West Bengal, 713209
INDIA

*Nomenclature*

J = Equivalent system mass moment of inertia about the central axis of the column referred to column motor shaft, kg-$m^2$.
$J_m$ = Column motor inertia referred to its own shaft, kg-$m^2$
$J_{col}$ = Column load mass moment of inertia about its own axis ( z-axis ), kg-$m^2$
$J_{col\text{-}eff}$ = Effective column mass moment of inertia referred to column motor shaft, kg-$m^2$
$M_{col}$ = Mass of column, kg
$M_{arm1}$ = Mass of arm1, kg
$M_{arm2}$ = Mass of arm2, kg
$M_{ee}$ = Combined mass of end-effector and payload, kg
$a_1$ = Distance of centre of gravity of arm1 from column rotational axis, m
$a_2$ = Distance of centre of gravity of arm2 from column rotational axis, m
$a_3$= Distance of centre of gravity of arm3 from column rotational axis, m
$T_{colM}$ = Column motor transfer function
$T_{colL}$ = Column load transfer function
B =Equivalent system viscous friction referred to column motor shaft, kg-m/rpm.
$B_m$ = Column motor viscous friction, kg-m/rpm.
$B_{col}$ = Viscous friction of the column, kg-m/rpm.
$B_{col\text{-}eff}$ = Effective viscous friction of the column, kg-m/rpm.
n = Column harmonic drive reduction ratio.
L= Inductance of column motor, H.
R = DC resistance of column motor, Ω.
$K_b$ = Column motor back e.m.f. constant, Volts/rpm.
$K_t$ = Column motor torque constant, kg-m/amp (rms).
$K_{P1}$ = Proportional gain of PID controller of position loop.
$K_{I1}$ = Integral gain of PID controller of position loop.
$K_{D1}$ = Derivative gain of PID controller of position loop.
$K_{P2}$= Proportional gain of PID controller of velocity loop.
$K_{I2}$ = Integral gain of PID controller of velocity loop.
$K_{D2}$ = Derivative gain of PID controller of velocity loop.

***Abstract***

The method of conventional control of a manipulator, without considering varying effects of robot dynamics, results in degraded response with unnecessary vibrations thus limiting the precision and speed of the end effector. As the column joint is subjected to worst dynamic conditions when all the axes are in motion, simulation of position response of column joint of a 60-Kg payload 4-axes SCARA type manipulator is presented by taking dynamical effect into consideration. The paper analyses dynamical effect on the basic control system by comparing the position response of the column joint, with and without considering the effects of robot dynamics, with PID controllers in the position as well as velocity loops as basic compensators. It has been found that dynamical effects on a SCARA type manipulator with a 60-Kg payload is very small and is suitable for pick and place type industrial applications.

## 1.0 Introduction

The conventional approach of using only robot kinematics for trajectory path planning renders inadequate control of manipulator especially if the manipulator payload is high. Treating each joint of the robot arm as a simple joint servomechanism of a manipulator results in degraded response with unnecessary vibrations, limiting the precision and speed of the end-effector.[1] A method of dynamic compensation of the joint torque is presented along

with a comparison of the position response of the system with and without considering dynamic model. The analysis is carried out by designing the control scheme of a 60 Kg payload SCARA type robot having 4 Degrees of Freedoms (DOFs). The robot can be controlled manually through control console / teach pendant or through the use of customised GUI in a supervisory computer. MATLAB's SIMULINK is used as the simulation tool for designing the control scheme and for analysis of positional response of joint.

## 2.0 The Robot System:

The photograph of the 4-axes robot manipulator with control console with specification given in **Table 1** is shown in **Fig. 1**.

**Fig. 1 Manipulator with control console**

## 3.0 Dynamic modeling:

The well known dynamical equations of a manipulator is given in eq.(1).[1] For the sake of simplicity of analysis, the rotation i.e orientation of end-effector, is neglected because this joint does not contribute much to the overall dynamic effect on the column joint.

$$\tau(t) = \mathbf{D}(\mathbf{q}(t))\ddot{\mathbf{q}}(t) + \mathbf{h}(\mathbf{q}(t),\dot{\mathbf{q}}(t)) + \mathbf{c}(\mathbf{q}(t)) \qquad (1)$$

From this relation, the dynamic torque equation for column or base axis of the manipulator, is given by eq.(2). In the equations, $Ji_{jk}$, for i = 1,..,4 ; j = 1,..,4 ; k = 1,..,4 represent elements of 4x4 pseudo-inertial matrices where the numbers 1,2,3 and 4 represents column, arm1, arm2 & end-effector respectively with sub-script notation representing correlation between two axes. Elements of inertia matrices are calculated using manipulator geometric configuration. In the analysis, the end-effector rotation $\theta_4$ is neglected. Elements of D matrix, h matrix and c matrix are calculated at each sample instant, corresponding to a defined straight-line path of end-effector by taking the reduction ratio into account, in order to reflect the dynamical torque on the column motor shaft. The schematic configuration of the manipulator is shown in **Fig. 2**.

$$\begin{aligned}\tau_1(t) = {} & D_{11}(t)\ddot{\theta}_1(t) + D_{12}\ddot{x}_2(t) + D_{13}(t)\ddot{\theta}_3(t) + h_{111}(t)\dot{\theta}_1^2(t) \\ & + h_{122}(t)\dot{x}_2^2(t) + h_{133}(t)\dot{\theta}_3^2(t) \\ & + (h_{112}(t) + h_{121}(t))\dot{\theta}_1(t)\dot{x}_2(t) \\ & + (h_{113}(t) + h_{131}(t))\dot{\theta}_1(t)\dot{\theta}_3(t) \\ & + c_1(t)\theta_1(t) + c_2(t)\theta_2(t) \qquad (2)\end{aligned}$$

where

$$\begin{aligned}D_{11}(t) = {} & J1_{11} + J2_{44} + J3_{11} + J3_{41}l_3 + J3_{14}l_3 + J3_{44}l_3^2 \\ & + (J3_{41} + J3_{44}l_3)l_2S_1S_{13} + (J3_{41} + J3_{44}l_3)l_2C_1C_{13} \\ & + J4_{11} + \{J4_{11}(l_3S_{13} + l_2S_1) + J4_{14}(l_3S_{13} + l_2S_1)\}S_{134} \\ & + \{J4_{11}(l_3C_{13} + l_2C_1) + J4_{14}(l_3C_{13} + l_2C_1)\}C_{134} \\ & + J4_{44}(l_3S_{13} + l_2S_1)^2 + J4_{44}(l_3C_{13} + l_2C_1)^2\end{aligned}$$

$$D_{12}(t) = J2_{44}$$

$$\begin{aligned}D_{13}(t) = {} & J3_{11} + J4_{11} + (J3_{44} + J4_{44})l_3^2 + (J3_{14} + J3_{41})l_3 \\ & + (J4_{14} + J4_{41})l_3C_4 + J4_{14}l_2C_{34} + J4_{44}l_2l_3C_3\end{aligned}$$

$$\begin{aligned}h1_{11} = {} & (J1_{11} + J1_{41}l_2)S_1 + (J3_{14} \\ & + J3_{44}l_2 - J2_{14} - J2_{44}l_2)l_3C_{13}S_{13} \\ & + (J3_{14} + J3_{44}l_2)l_2C_{13}S_1 - (J2_{14} + J2_{44}l_2)l_2C_1S_{13}\end{aligned}$$

$$h1_{12} = J2_{44}$$

$$h1_{12} = -(J3_{11} + J3_{14}l_3)S_4 - J4_{14}l_2S_{34}$$

$$h1_{21} = J2_{44}$$

$$h1_{31} = J4_{11}S_3$$

$$h1_{33} = J4_{11}S_3 + J4_{14}l_2(S_3C_4 - C_3S_4) - J4_{14}l_2S_4$$

$$c1 = Marm1g$$

$$c2 = (Marm1 + Marm2 + Mee)g$$

## 4.0 Formulation and simulation of robot control scheme:

Standard PID control principle is utilised to develop the overall robot control scheme through position response simulation and analysis at each sampling instant. Position mode control is used which

encapsulates velocity, as well as current / torque control. The current loop of the controller receives feedback from current sampling circuitry using closed-loop Hall sampling techniques. The current sample is used by the current loops to regulate the current in each of the three motor phases. The absolute motor current is invoked through actuator-level motion control software, which is interfaced to the robot control foreground program for position control.

### 4.1 Kinematic formulation and trajectory planning for rectilinear movement of the tool co-ordinate system

The control problem starts with trajectory planning, i.e. the pre-defined path to be followed by the end-effector within a desired time in the world space. The entire path is broken down into small segments to be traversed in small time intervals. All the joints are actuated in such co-ordinated manner that the resultant end effector motion in the world co-ordinate system is maintained [6]. The end-effector follows a trapezoidal velocity profile where the position of the end-effector at time t=0 is $[p_x(0),p_y(0),p_z(0)]$and at time $t=t_f$ is $[p_x(t_f),p_y(t_f),p_z(t_f)]$. The acceleration time $t_a$ and deceleration time $t_d$ of the end-effector is determined from the characteristics of the motors and the servo-amplifiers located at each joint for the end-effector motion. Since the distance travelled by the end-effector is equal to the integral of the velocity over time, the area of the trapezoid equals the distance between the initial and terminal points of a path followed by the end-effector. [2]

The simultaneous movements of column ($\theta_1$), arm1 ($x_2$) and arm2 ($\theta_3$) joints is considered and torque required by the column motor is calculated, as the dynamic effects on column joint is much pre-dominant when the column itself and other arms are moving. The analysis is simplified by neglecting the end-effector orientation ($\theta_4$) as this do not affect the rectilinear motion of column joint. We have assumed that the manipulator end-effector is to move from the home position at (1500 mm, 0, 1500 mm) to a final position at (750 mm, 750 mm, 2600mm) in the world co-ordinate frame. Hence, the planar and vertical motion is followed using the trapezoidal velocity profile as stated above. The maximum velocity, acceleration time $t_a$ and deceleration time $t_d$ of the end-effector for planar motion are chosen as 2m/sec., 200 msec and 200 msec respectively, while the corresponding values for the vertical motion are 1m/sec, 200 msec and 200 msec. This assumption is based on the characteristics of individual motors and servo-amplifiers included in the system.

In the trajectory planner, the joint positions are calculated using inverse kinematics model. Using MATLAB, the $[T_1, \theta_1]$ matrix is generated. $T_1$ is the time vector consisting of time elements starting from t=0 up to a time $t = t_{f1}$ second, the sampling interval being 0.02 second, and $\theta_1$ is the column position vector consisting of elements representing column joint position at each sampling instant. The positional deviation of column joint at each sampling instant represented by $\Delta\theta_1$ is calculated from the elements of $\theta_1$ vector. Similarly, $[T_1, \theta_3]$ matrix is generated which represents the time vs. position information for arm2 joint, $\Delta\theta_3$ being the positional deviation of arm2 joint at each sampling instant. In the same manner, $[T_2, x_2]$ matrix represents the time vs. position information for arm1 joint, where $T_2$ is the time vector consisting of time elements starting from t=0 up to a time $t = t_{f2}$ second. The D, h and c terms of eq. (1) are calculated using the values of elements of inertia matrices given in **Table 2** and **Table 3**, $\theta_1$, $x_2$ and $\theta_3$.

### 4.2 Simulation of column position response

The position control scheme was developed step-by-step using MATLAB. The basic robot control scheme using PID controller was designed using SIMULINK [6]. In **Fig. 3** and from **Table 2**, the column motor transfer function is given as

$$T_{colM} = 1/(Ls+R) = 1/(0.0441s+2.05) \quad (3)$$

and the column load transfer function is given as

$$T_{colL} = 1/(Js+B) = 1/(0.2746s+0.018x10^{-4}) \quad (4)$$

Where $J = J_m + J_{col\text{-}eff} = J_m + (1/n)^2 * (J_{col} + M_{arm1} * a_1^2 + M_{arm2} * a_2^2 + M_{ee} * a_3^2) = 0.106$ kg-m$^2$

$B = B_m + B_{col\text{-}eff} = B_m + (1/n^2) B_{col} = 0.018x10^{-3}$ Nm/rpm , where $B_{col}$ is negligible

The position parameters derived from robot kinematics at each sampling instant for column joint forms the starting block of the control scheme. The PID gain parameters ($K_P$, $K_I$, $K_D$) in position and velocity loops are adjusted in order to tune the system for achieving desired transient and steady state response. The closed-loop transfer function of the control system for the column joint shown in **Fig. 3** is as follows: [3] [4]

$$\theta_0(s) / \theta_d(s) = a / b \quad (5)$$ where

$$a = s^2 (K_{P1} + K_{I1} / s + s K_{D1}) (K_{P2} + K_{I2} / s + s K_{D2}) K_b K_t \quad (6)$$

$$b = cs^5 + d s^4 + e s^3 + f s^2 + g s + h \quad (7)$$ where

$c = JL$

$d = BL + JR + K_{D1}K_{D2}K_b K_t$

$e = BR + (1 + K_{D2} + K_{P1}K_{D2} + K_{D1}K_{P2})K_b K_t$

$f = (K_{P2} + K_{P1}K_{P2} + K_{I1}K_{P2} + K_{D1}K_{I2})K_b K_t$

$g = (K_{I2} + K_{P1}K_{I2} + K_{I1}K_{P2})K_b K_t$

$h = K_{I1}K_{I2}K_b K_t$

With reference to **Table 2**, the characteristic equation of the closed loop system is denominator polynomial of equation (5), as given by equation (7). As is evident from equation (7), it is a fifth order system. The roots of equation (7) determine the closed loop poles of the system, the system behaviour being approximately characterised by the location of dominant poles in s-plane [5]. Solving equation (7) using values of position loop and velocity loop PID controllers gain parameters ($K_{P1}$= 200, $K_{I1}$ = 10, $K_{D1}$= 15 and $K_{P2}$= 1000, $K_{I2}$ = 200, $K_{D2}$= 8), yields values for the poles as $s_{1,2} = -1.923 \pm j\,0.8438$, $s_3 = -0.1425$, $s_4 = -0.0019$, $s_5 = -0.0005$ which shows the system is stable.

In order to mimic the real situation, the control system of **Fig. 3** is modified for incorporating dynamic effect on the system in **Fig. 4** The blocks depicting various components of dynamical torques in **Fig. 4** consist of several small sub-blocks, which are masked for clarity.

A compensation scheme for neutralizing the dynamic effect for better response is given in **Fig.5**. In this case, actual motor current is read through low-level motion control software supplied with servo-amplifiers. This current information is converted into torque information through the use of torque constant, $K_t$. This torque is subtracted from the dynamical torque required, calculated off-line for all sampling instants. The additional torque demand $\Delta\tau$ is converted to equivalent motor voltage and is fed forward with the output of velocity loop PID controller.

## 5.0 Simulation Results and Discussion

The desired response curve of column joint at each sampling instant is given in **Fig. 6**. Simulation curves related to the basic control scheme in **Fig. 3** are shown in **Fig. 7(a)** and **Fig. 7(b)**, where effect of variation of PID gain parameters are shown. The response can be improved by adjusting values of PID1 and PID2 gain parameters. Keeping the values of the gain parameters of velocity loop PID controller fixed at $K_{P2}$ = 300, $K_{I2}$ = 100 and $K_{D2}$ = 2, the gain adjustments on PID1 controller is carried out. Keeping the values of $K_{I1}$ and $K_{D1}$ fixed at 10 and 2 respectively, it is observed that a value of $K_{P1}$ = 200 yields optimum result. As $K_{P1}$ increases, oscillation and ringing increases while steady error slightly reduces. If the value of $K_{P1}$ exceeds 5000, the response is oscillatory. If $K_{P1}$ decreases from 200, overshoot and ringing increases. Now the value of $K_{I1}$ is adjusted keeping $K_{P1}$ and $K_{D1}$ fixed at 200 and 2 respectively. It is seen that with the increase of $K_{I1}$ the steady-state error decreases but the oscillation increases as expected. It is observed that the system is comparatively immune to the adjustment of values of $K_{I1}$ for a large range except for significant reduction of steady state error observed from about 1500. Keeping $K_{P1}$ and $K_{I1}$ fixed at 200 and 10 respectively, the behaviour of response is studied where an increase of $K_{D1}$ reduces peak overshoot, oscillation and increases steady state error up to a value of about 50, beyond which the output exhibits limit cycle. In fact, a lower value of $K_{D1}$ is desired in order to reduce steady–state error. Also, addition of derivative control, with characteristics of a high-pass filter, tends to propagate noise and disturbances through the system. In fact, a lower value of $K_{D1}$ is desired in order to reduce steady–state error. The fine tuning of PID1 gain parameters results in desired transient response. Using above observations, PID1 block is fine tuned, response behaviour noted and then PID2 block is fine-tuned as shown in **Fig. 7(a)** and **Fig. 7(b)**. In **Fig. 7(a),** $K_{P1}$ = 200, $K_{I1}$ = 10, $K_{D1}$ = 2 and $K_{P2}$ = 300, $K_{I2}$ = 100, $K_{D2}$ = 2 while in **Fig. 7(b)** $K_{P1}$ = 1000, $K_{I1}$ = 500, $K_{D1}$ = 8 and $K_{P2}$ = 1000, $K_{I2}$ = 500, $K_{D2}$ = 5, the response in **Fig. 7(b)** being optimum.

The basic position control system is modified as shown in **Fig. 4** to account for the dynamical effects on the column axis when the column, arm1 and arm2 are in motion. The response curve is shown in **Fig. 7(c)**. It is observed that the system, using the same gain parameters of PID1 and PID2 controllers as that of the basic system, is subjected to overshoots at transitions of velocity profile, ringing and steady-state error at each sampling instant and is thus relatively unstable. As the modified system does not add any additional pole or zero to the basic system, its absolute stability is guaranteed. For reducing the values of overshoots, ringing etc. in the transient response, the modified system with dynamic compensation as represented by **Fig. 5** is proposed. It has been observed that the undesirable system response has improved as that of the basic system keeping the same values of gains of PID1 and PID2

controllers. The response of the compensated system with the same values of gain parameters is shown in **Fig. 7(d)**. The system can be further tuned for optimum transient and steady state response by adjusting the values of gain parameters.

## 6.0 Acknowledgement

The project members of this project express their sincere gratitude and thanks to the Director, CMERI for his co-operation and assistance and encouragement to make the developmental work successful.

*References & Bibliography*

1. K.S. Fu, R.C. Gonzalez and C.S.G. Lee, Robotics: Control, Sensing, Vision and Intelligence, McGraw-Hill, pp12-265.
2. A.J. Koivo, Fundamentals for Control of Robotic Manipulators, Wiley & Sons Inc., pp 35-178, pp 227-297.
3. Karl J. Astrom and Bjorn Wittenmark, Computer-Controlled Systems, Prentice Hall, pp 209-230.
4. Gene F. Franklin, J. David Powell, Abbas Emami-Naeini, Feedback Control of Dynamic Systems, Addison-Wesley, pp 442-576.
5. Benjamin C. Kuo, Automatic Control Systems, Prentice Hall, pp 259-367.
6. R. Featherstone, " Position & Velocity Transformation between Robot End-Effector Coordinates and Joint Angles," Internation Journal of Robotics Research, Vol. 2, No. 2, Summer 1983
7. M. Tarokh and H. Seraji, "A Control Scheme for Trajectory Tracking of Robot Manipulators," Proceedings, 1988 IEEE International Conference on Robotics & Automation, pp 1192 - 1197.
8. A.K. Bejczy, T.J. Tarn, Y.L.Chen," Robot Arm Dynamic Control," Proceedings, 1985 IEEE International Conference on Robotics & Automation.

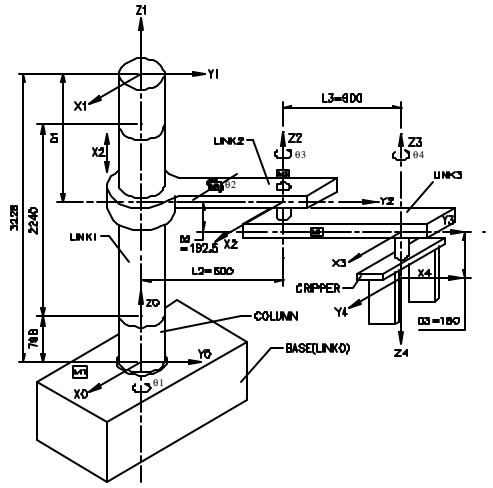


**Fig. 2 Schematic configuration of the manipulator**

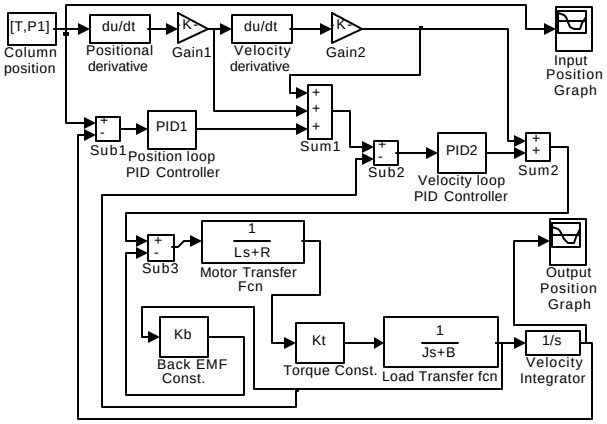


**Fig. 3 Basic position control system with PID controllers**

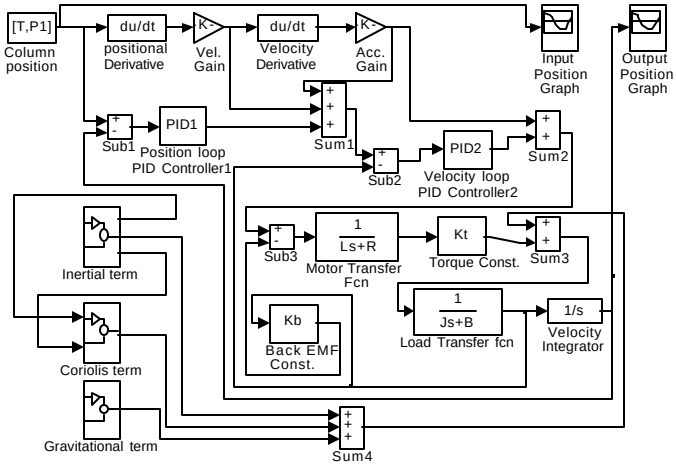


**Fig. 4 Position control system with dynamic effects**

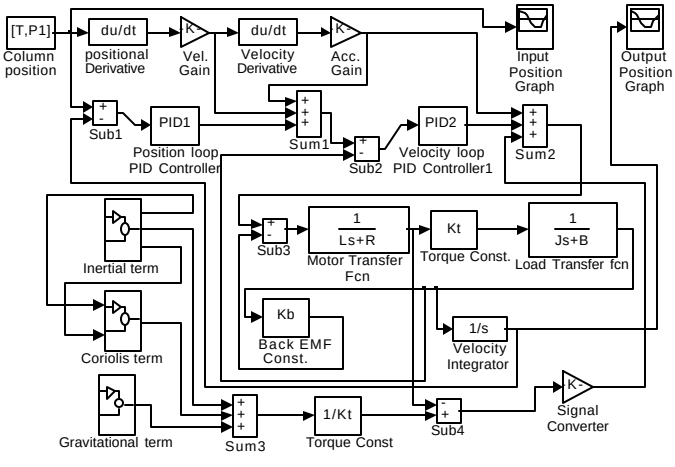


**Fig. 5 Position control system with dynamic compensator**

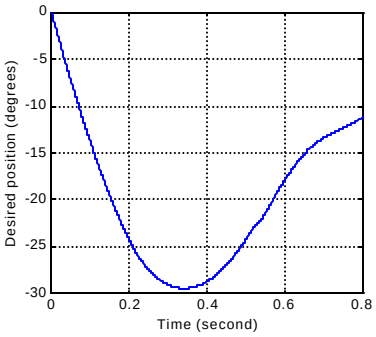


**Fig. 6 Desired response**

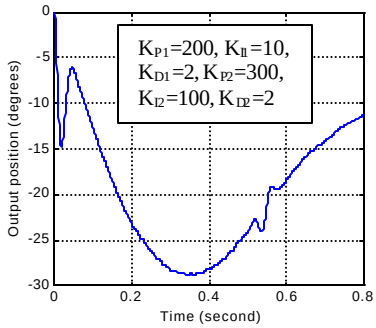


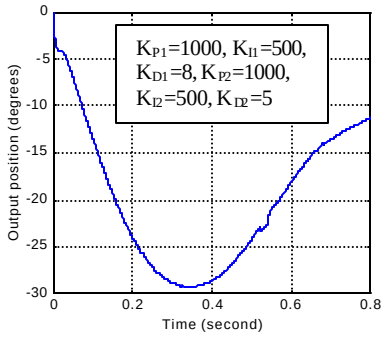


**Fig. 7(a) & (b) Position response without dynamic effects**

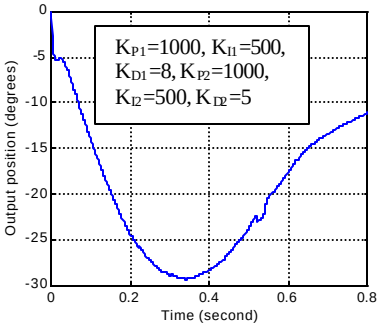


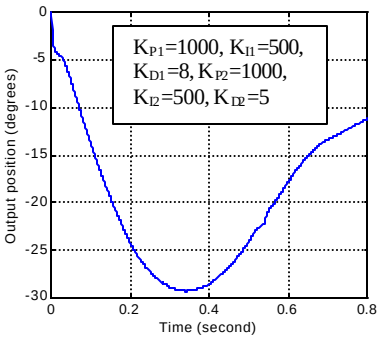


**Fig. 7(c) & (d) Position response with dynamic effects & compensation**

| Configuration | SCARA type |
|---|---|
| Payload | 60 kgs. |
| Degrees of freedom | 4 |
| Rotation of Column | 400-450 deg. |
| Velocity of Column | 120-160 deg/sec |
| Linear travel of Arm1 | 1.5-2 m. |
| Tip speed | 0.75-1m/sec. |
| Rotation of Arm2 | 260-300 deg. |
| Velocity of Arm2 | 120-160 deg/sec |
| Rotation of End Effector | 450-600 deg. |
| Velocity of End Effector | 180-400 deg/sec |

**Table 1**

| **Axis parameters** | **Column** | **Arm1** | **Arm2** | **End Effector** |
|---|---|---|---|---|
| Motor Kilowatts | 2 | 1.8 | 0.97 | 1.0 |
| Motor Rated speed (rpm) | 1500 | 2800 | 1500 | 3800 |
| Motor continuous torque (Nm) | 13. | 6.24 | 6.8 | 2.44 |
| Motor continuous line current (amps.) | 6 | 6.0 | 3.0 | 3.0 |
| Motor max line-to-line voltage (volts) | 250 | 250 | 250 | 250 |
| Motor DC resistance at 25deg line-to-line (R, ohms) | 4.10 | 2.32 | 10.54 | 6.98 |
| Motor inductance line-to-line (L, mH) | 102 | 32 | 220 | 68 |
| Motor mass moment of inertia ($J_m$, kg-$m^2$ ) | 0.000656 | 0.000251 | 0.000323 | 0.0001 |
| Motor viscous damping ($B_m$, Nm/krpm) | 0.018 | 0.012 | 0.015 | 0.007 |
| Motor torque constant ($K_t$, kg-m/amps) | 0.231 | 0.1077 | 0.252 | 0.081 |
| Motor back emf constant ($K_b$, V/rpm) | 0.140 | 0.065 | 0.136 | 0.049 |
| Mass moment of inertia about own axis (kg-$m^2$.) | 9.32 | 10.56 | 16.2 | 0.53 |
| Mass of axis (M, kg) | 750 | 88 | 60 | 80 |
| Distance between each successive axes(l, m) | 0.0 | 0.6 | 0.9 | 0.2 |
| Distance of c.g. of each axis from column axis (m) | 0.0 | 0.3 | 1.05 | 1.5 |
| Reduction ratio (n) | 50 | 13 | 50 | 50 |

**Table 2**

| Servoamplifier | Column | Arm1 | Arm2 | End Effector |
|---|---|---|---|---|
| Main input (DC volts) | 125-360 | 125-360 | 125-360 | 125-360 |
| Rated Power (DC KW) | 1.26-2.79 | 1.26-2.79 | 0.63-1.4 | 0.63-1.4 |
| Cont. power @ 230V ac 3-ph line (KVA) | 2.2 | 2.2 | 1.1 | 1.1 |
| Continuous current (Amps) | 6.0 | 6.0 | 3.0 | 3.0 |
| Analog input range (Volts) | -10V to +10V. | -10V to +10V. | -10V to +10V. | -10V to +10V. |

**Table 3**